Dissociation of circadian and light inhibition of melatonin release through forced desynchronization in the rat

Michael D. Schwartz[a,1], Cheryl Wotus[a,2], Tiecheng Liu[b], W. Otto Friesen[c], Jimo Borjigin[b,3], Gisele A. Oda[d,3], and Horacio O. de la Iglesia[a,3]

[a]Department of Biology and Program of Neurobiology and Behavior, Box 351800, University of Washington, Seattle, WA 98195; [b]Department of Molecular and Integrative Physiology, University of Michigan Medical School, Ann Arbor, MI 48109; [c]Department of Biology, University of Virginia, Charlottesville, VA 22903; [d]Instituto de Biociências, Departamento de Fisiologia, Universidade de São Paulo, Cidade Universitária 05508-900, São Paulo, SP, Brazil

Edited by Joseph S. Takahashi, Northwestern University, Evanston, IL, and approved August 19, 2009 (received for review June 16, 2009)

Pineal melatonin release exhibits a circadian rhythm with a tight nocturnal pattern. Melatonin synthesis is regulated by the master circadian clock within the hypothalamic suprachiasmatic nucleus (SCN) and is also directly inhibited by light. The SCN is necessary for both circadian regulation and light inhibition of melatonin synthesis and thus it has been difficult to isolate these two regulatory limbs to define the output pathways by which the SCN conveys circadian and light phase information to the pineal. A 22-h light–dark (LD) cycle forced desynchrony protocol leads to the stable dissociation of rhythmic clock gene expression within the ventrolateral SCN (vlSCN) and the dorsomedial SCN (dmSCN). In the present study, we have used this protocol to assess the pattern of melatonin release under forced desynchronization of these SCN subregions. In light of our reported patterns of clock gene expression in the forced desynchronized rat, we propose that the vlSCN oscillator entrains to the 22-h LD cycle whereas the dmSCN shows relative coordination to the light-entrained vlSCN, and that this dual-oscillator configuration accounts for the pattern of melatonin release. We present a simple mathematical model in which the relative coordination of a single oscillator within the dmSCN to a single light-entrained oscillator within the vlSCN faithfully portrays the circadian phase, duration and amplitude of melatonin release under forced desynchronization. Our results underscore the importance of the SCN's subregional organization to both photic input processing and rhythmic output control.

circadian desynchronization | dual oscillators | suprachiasmatic

In mammals, circadian rhythms are governed by a master pacemaker located in the hypothalamic suprachiasmatic nucleus (SCN) (1, 2). The SCN is a heterogeneous nucleus with major subregional differences in neurochemical phenotype, connectivity and patterns of gene expression (3–6). Light information is transmitted directly to the SCN via the retinohypothalamic tract (RHT) (7, 8). In rats, RHT input is dense in the ventrolateral SCN (vlSCN), and relatively sparse in the dorsomedial SCN (dmSCN) (3). In this species, segregation of SCN afferents is paralleled by a segregation of efferent projections emerging from each subregion, and some SCN targets receive input from only the vl- or the dmSCN (9). This topographic organization of afferent and efferent projections suggests different roles for these subregions regarding processing of photic information and control of circadian outputs. Indeed, photic stimulation by light pulses applied during the subjective night or by abruptly shifting the light–dark (LD) cycle up-regulates expression of the clock gene *Per1* in the vlSCN, inducing a transient desynchronization in gene expression between the two subregions (10–13). These data strongly suggest that the SCN's subregional organization is key to the processing of light information. Its role in the control of circadian outputs, however, is more difficult to assess and has been limited to studies using partial SCN lesions (14).

We have recently developed a forced desynchrony protocol in rats that leads to stable dissociation between the vl- and dmSCN. When housed in symmetrical 22-h 11:11 LD cycles (LD22), rats exhibit two stable locomotor activity rhythms simultaneously: One is entrained to the LD cycle and exhibits a period of 22 h (T22), whereas the other is dissociated from the LD cycle and presents a period longer than 24 h ($\tau > 24$) (15, 16). Over time, these bouts move between aligned phases, in which the $\tau > 24$ bout occurs during the dark phase of the LD cycle (and thus overlaps the T22 activity bout), and misaligned phases, in which the $\tau > 24$ bout occurs during the light phase (and thus overlaps with the T22 rest phase). The T22 and $\tau > 24$ activity rhythms are correlated with independent oscillations in clock genes in the vlSCN and dmSCN, respectively. We have confirmed this dissociation in rhythmic clock gene expression for the *Per1*, *Per2*, and *Bmal1* genes (16, 17) and *ex vivo* in hypothalamic slices of desynchronized rats carrying a luciferase gene driven by the *Per1* promoter (unpublished data). Although the oscillation of *Per1* expression in the vlSCN is associated with the 22-h LD cycle, high expression of *Per1* during the light phase does not represent solely a photic response because it persists upon release into constant darkness (DD) (16). Furthermore, desynchronization of other circadian rhythms (16–18) indicates that the forced desynchronized rat represents a unique anatomically and genetically intact model to study the respective contributions of the dm- and vlSCN to specific behavioral and physiological rhythmic outputs (19).

The rhythmic release of the pineal hormone melatonin was characterized as an SCN circadian output more than three decades ago (20). Its tight nocturnal release pattern is the result of both circadian control and light-inhibition of its synthesis (21) and the SCN is critical for both of these regulatory processes (20, 22). The SCN exerts this regulation via a multisynaptic projection that originates in the nucleus and has synaptic relay stations in the paraventricular nucleus of the hypothalamus (PVN), the intermediolateral cell column of the spinal cord and the superior cervical ganglion, whose projections terminate in the pineal gland (23, 24). In the rat, output signals from the SCN regulate levels of mRNA for pineal arylalkylamine N-acetyltransferase (AANAT), a key enzyme in the melatonin synthesis pathway. Nocturnal up-

Author contributions: M.D.S., C.W., J.B., and H.O.d.l.I. designed research; M.D.S., C.W., T.L., J.B., and H.O.d.l.I. performed research; J.B. contributed new reagents/analytic tools; M.D.S., C.W., W.O.F., J.B., G.A.O., and H.O.d.l.I. analyzed data; G.A.O and W.O.F. developed mathematical model; and M.D.S., C.W., W.O.F., J.B., G.A.O., and H.O.d.l.I. wrote the paper.

The authors declare no conflict of interest.

This article is a PNAS Direct Submission.

[1]Present address: Department of Pharmacology and Experimental Therapeutics, University of Maryland, School of Medicine, Baltimore, MD 21201.

[2]Present Address: Department of Biology, Seattle University, Box 222000, Seattle, WA 98122-1090.

[3]To whom correspondence may be addressed. E-mail: borjigin@umich.edu, gaoda@ib.usp.br, or horaciod@u.washington.edu.

This article contains supporting information online at www.pnas.org/cgi/content/full/0906382106/DCSupplemental.

regulation of AANAT mRNA is the main cause for the 150-fold increase in melatonin synthesis during the night (25, 26).

Light is the most prevalent environmental stimulus that synchronizes the SCN circadian pacemaker; in addition, light exerts direct effects on many of the pacemaker's rhythmic outputs, including melatonin release. Therefore, it has been difficult to experimentally separate the acute inhibitory effects of light on melatonin synthesis from those mediated through light entrainment of the SCN pacemaker (27). Here, we show that entrainment of the circadian rhythm of release of melatonin can indeed be dissociated from its light-inhibition by exposure of rats to LD22. Our present results, in combination with our clock gene expression patterns under LD22 published in refs. 16 and 17, indicate that light input relayed by the vlSCN directly to the pineal is likely the source of acute photic inhibition of melatonin synthesis and release. In other words, although light under LD22 fails to fully entrain the dmSCN, it never fails to inhibit melatonin. Furthermore, the circadian release of melatonin under this desynchrony protocol reflects the failure of the dmSCN to entrain to the continuously advancing 22-h LD cycle. Our results fit the predictions of a dual oscillator model in which the vl- and dmSCN are mutually but asymmetrically coupled oscillators. According to this model, light entrains the vlSCN; under 24-h LD cycles the two oscillators are synchronized by coupling exerted by the vl- on the dmSCN and this synchronization is impaired by exposure to LD22.

Results

Desynchronization of Melatonin Release Under 22-h LD Cycles. Male Wistar and Kyoto–Wistar (Kyoto) rats ($n = 8$ for each strain) were housed in LD22. Visual inspection of actograms indicated desynchrony in all animals. In Wistar rats this was manifested as two locomotor bouts, one associated with the LD cycle and the other dissociated from it as described in refs. 15 and 16 (Fig. 1*A*). In Kyoto rats the desynchrony was manifested as locomotor activity bouts that advanced on successive cycles, but failed to achieve the 2-h advance per cycle needed to entrain to the LD cycle (Fig. 1*B*). χ^2 periodogram analysis revealed two peaks in the circadian range for all individuals in both strains. The mean periods for Wistar rats were $T = 22.00 \pm 0.00$ h and $\tau = 25.32 \pm 0.11$ h corresponding to the T22 and $\tau > 24$ bouts, respectively. The mean periods for Kyoto rats were $T = 22.06 \pm 0.01$ h and $\tau = 24.08 \pm 0.03$ h. In this periodogram analysis the T22 period explained a significantly greater percentage of the variance in Wistar than in Kyoto rats; furthermore, the $\tau > 24$ period showed a higher peak in Kyoto than in Wistar rats ($F_{(1, 11)} = 23.7$, $P = 0.0004$).

Animals were implanted with microdialysis probes aimed at the pineal and melatonin levels were monitored from dialysates with a 20-min sampling interval. Melatonin release duration was maximal when the $\tau > 24$ bout overlapped with the dark phase of the LD cycle (Figs. 1 and 2 *A* and *C*). As the $\tau > 24$ bout progressed from aligned to misaligned phases the duration of the melatonin peak gradually decreased. Thus, melatonin peak duration was negatively correlated with the number of days past the aligned phase (Fig. 2 *B* and *D*) ($r = -0.738$, $P < 0.001$ for Wistar rats and $r = -0.806$, $P < 0.001$ for Kyoto rats). This compression of the melatonin peak duration was more rapid in Wistar than in Kyoto rats (3–5 days versus 5–7 days) (Figs. 1 and 2).

Compression was also associated with differential rates of advance for melatonin onset and offset from aligned to misaligned phases. For Wistar rats, the periods of melatonin release onset and offset (determined as the times when melatonin levels reached respectively higher and lower values than the 20% of the daily peak) were respectively 23.21 ± 0.09 h and 21.86 ± 0.10 h. For Kyoto rats, these periods were respectively 23.50 ± 0.28 h and 21.96 ± 0.06 h. During maximum misalignment, melatonin was entirely suppressed for at least one cycle; during these periods of suppression, pineal *N*-acetylserotonin (enzymatic product of AANAT) was also suppressed, while pineal serotonin (precursor of melatonin and substrate for AANAT) levels were persistently elevated, ruling out a failure in sampling as a cause for loss of melatonin signal. The melatonin peak then reappeared near the next aligned phase, and the pattern repeated itself (Fig. 1). The onset of this reemerged melatonin release bout maintained a 1–2 h lag relative to lights-off for several days before resuming the compression pattern; the offset either phase-locked to the time of lights-on immediately upon reappearing, or initially appeared in the mid-dark phase and then phase-locked to lights-on after 1–2 cycles (Fig. 2 *A* and *C*). Thus, melatonin offset was tightly coupled to lights-on, whereas melatonin onset was neither phase-locked to the LD cycle nor fully free-running.

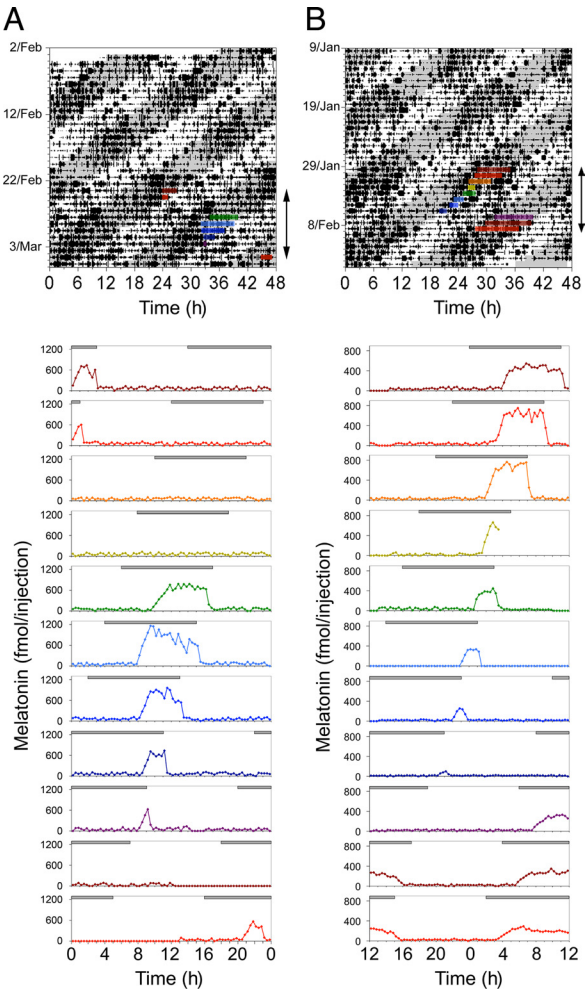

Fig. 1. Forced desynchronization of melatonin release. (*Upper*) Representative double-plotted actograms showing cage locomotor activity and the times (arrows) at which pineal melatonin was sampled through microdialysis in a Wistar rat (*A*) and a Kyoto rat (*B*) under a LD22. Color bars represent times when melatonin levels were above the 20% of the daily maximum. (*Lower*) Single-plotted daily melatonin profiles of the same animals shown on top. The color of each profile corresponds to the color of each melatonin release bout shown on the actogram above. Gray lines at the top of each melatonin profile indicate the dark phase of the LD cycle. Melatonin concentrations are not normalized and are reported as femtomoles per injection.

Compression of the Rhythm of Melatonin Release Reflects the Entrainment of a Slow-Advancing Oscillator. The melatonin peak compression observed in the transition from aligned to misaligned phases results in part from the time of lights-on impinging on nocturnal release of melatonin. This compression could either reflect the direct inhibition of melatonin synthesis by light or the

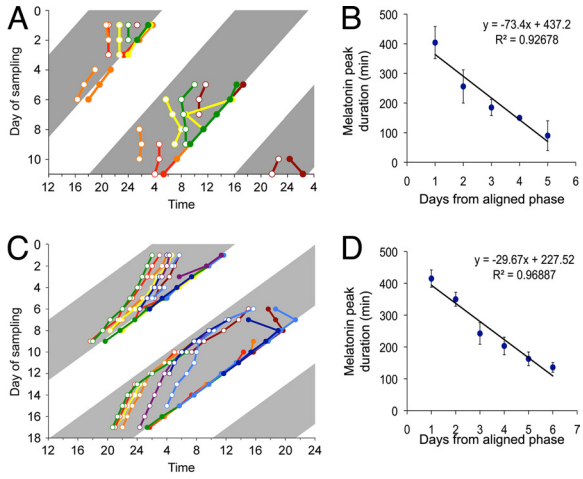

Fig. 2. Compression and decompression of melatonin release peaks under 22-h forced desynchronization. Double-plotted daily melatonin onset (open circles) and offset (colored circles) for Wistar (*A*) and Kyoto–Wistar rats (*C*) kept in LD22. Each color represents a single animal. Time scales are extended to better visualize the pattern of melatonin release. (*B* and *D*) average melatonin peak duration as a function of phase alignment; day 0 is the day of maximum alignment between the vl- and dmSCN. Values represent the mean ± SEM daily melatonin peak duration in minutes for all individuals.

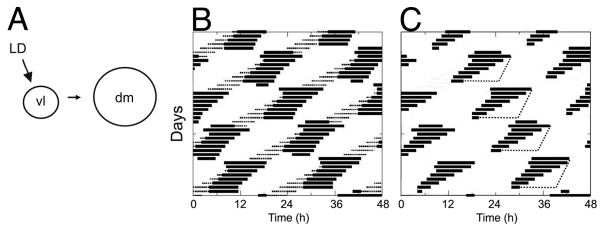

Fig. 3. Simulations of melatonin release as the output of the vl- and dmSCN under a forced desynchrony protocol. (*A*) Schematic diagram of proposed decoding of LD input by SCN subregions. Light entrains the vl oscillator within the vlSCN directly and the dm oscillator within the dmSCN indirectly through coupling between vl and dm oscillators. Relative size of the circles indicates relative period (τ) values for the oscillators. (*B*) Simulation of two coupled vl (thin line) and dm (heavy line) oscillators shown schematically in *A*. The vl oscillator is entrained to Zeitgeber $T = 22$, while dm oscillator is in relative coordination; melatonin production is controlled by the dm oscillator. (*C*) Masking of melatonin release (dotted line) by light, relayed through the vlSCN, is added to the system, and the output of the vlSCN is removed. Parameters for F, G: $\tau_V = 23$ ($a_v = 0.85$; $b_v = 0.3$; $c_v = 1.1$; $d_v = 0.5$); $\tau_d = 24.3$ ($a_d = 0.85$; $b_d = 0.3$; $c_d = 0.75$; $d_d = 0.5$); $C_{vd} = 0.14$; $L_{dur} = 11$ h; $L = 1$; LD period $T = 22$ h.

entrainment of an oscillator by the advancing 22-h LD cycle. To sort out between these possibilities, we released male Wistar rats into DD after 14 days under the 22-h desynchrony protocol by leaving the lights off at the conclusion of the dark phase. Based on locomotor activity data, three animals were determined to be in aligned phase at the time of release (Fig. S1*A*, C). In these animals, both melatonin onset and offset free-ran from the point of release, with a period of 24.44 ± 0.08 h and 24.49 ± 0.10 h, respectively. As expected, the melatonin peak duration in these individuals was long from the first day in DD onward. The remaining two animals were in misaligned phase at the time of release into DD (Fig. S1 *B* and *C*). In both of these animals, the first melatonin peak in DD was compressed. In one case, the melatonin peak expanded via small daily advances in onset (Fig. S1 *B* and *C*). In the other case, the melatonin peak delayed sharply on the second day in DD, then expanded via further delay of offset (Fig. S1C). The probe signal was lost in this animal after the third day in DD, but the available data demonstrate an initially compressed melatonin peak that, on the second day in DD, appeared to initiate a phase jump similar to those seen in LD22. Thus, compression of the melatonin peak under LD22 cannot be explained merely as inhibition of melatonin release by light.

A Model for Light-Inhibition and Circadian Regulation of Melatonin Release by SCN Subregional Oscillators. The temporal patterns of melatonin release under forced desynchronization resemble locomotor activity patterns described by Pittendrigh and Daan (28, 29). In their research on nocturnal rodents exhibiting relative coordination under *T* cycles (cycles of periodic light pulses), periodic compression and decompression of activity duration were interpreted as the differential entrainment of individual oscillators controlling the onset and offset of activity. The duration of melatonin synthesis has also been proposed to be under control of two coupled oscillators (30, 31). Using computer simulations (see *Model Equations* in *SI Text*) we show that two oscillators (vl and dm) can explain our forced desynchronization results, but only one of them is sufficient for explaining compression and decompression of melatonin release.

For a configuration in which a Zeitgeber of fixed amplitude acts on two mutually coupled oscillators, A and B, the dynamics depend on the relationship between Zeitgeber period *T*, the intrinsic periods of the oscillators, τ_A and τ_B, the range of entrainment of each oscillator and the coupling strength (see *Simulation of Forced Desynchronization* in *SI Text* and Fig. S2). Simulation of a system exhibiting a simpler structural configuration, and based in the rat SCN topographical organization (3, 10, 18) (Fig. 3*A*) generates similar dynamics to those shown for the more general system in Fig. S2*A*. Therefore, the principles that underlie forced desynchronization of a dual oscillator system, in which light acts on both oscillators, apply to the more specific model in which the vl- and dmSCN are the coupled oscillators and light acts only on the vlSCN.

Forced Desynchronization Model of Melatonin Release. A population of oscillators with differing intrinsic periods can give rise to different emergent output patterns depending on whether they are mutually or unidirectionally coupled (32–34). In the SCN, there is a complex coupling architecture among neurons with different intrinsic circadian periods (4, 35, 36). This architecture gives rise to locally organized subpopulations of neuronal oscillators that are synchronized under 24-h LD cycles but may be dissociated under forced desynchrony protocols if their emergent periods are intrinsically different (15). The regulation of clock outputs and the pattern of clock gene expression in our LD22 forced-desynchronized rat clearly indicate that the vl- and dmSCN are functionally distinct neuronal subpopulations with distinct intrinsic periods (15, 16, 18). These and other results in rats and mice (10, 13, 37, 38) have led to the notion that the LD cycle entrains an oscillator in the vlSCN that in turn entrains the dmSCN (Fig. 3*A*).

When melatonin release is assayed under LD22, a pattern arises (Fig. 1) that does not resemble a typical dissociated locomotor activity pattern. In our model, whereas locomotor activity is the output of both the vl- and dmSCN, melatonin is controlled by the dmSCN (dm oscillator) (see *Model Equations* in *SI Text* for rationale behind these assumptions). The dm oscillator has a period $\tau_{dm} > 24$ h, whereas the period of the vlSCN (vl oscillator) is $\tau_{vl} < 24$ h. These periods are based on our previous analysis of clock gene expression and locomotor activity rhythms in desynchronized rats and on the fact that a 22-h LD cycle is within the limits of entrainment of the vlSCN but outside the limits of entrainment of the dmSCN (16). The pattern of melatonin release is proposed to correspond to the simulation case in which $T = T_2$ in Fig. S2: The 22-h LD cycle entrains the vl oscillator while the dm oscillator is in relative coordination (Fig. 3*B*).

Acute inhibition by light is superposed onto the simulated melatonin release in Fig. 3*C*, by setting melatonin amplitude to zero

for 11 h on a 22-h period basis, at an arbitrarily chosen initial phase. This simple procedure generates a melatonin output pattern that reproduces the main features of experimental data (compare Figs. 1 and 2 with Fig. 3*C*), namely slowly drifting melatonin onset times relative to LD 11:11, appropriately timed phase jumps and a 22-h period for melatonin offset. Because the vlSCN expresses a 22-h periodicity we propose it mediates the inhibition of melatonin by light and it relays photic information to the dmSCN. The dm oscillator is in relative coordination and, accordingly, its period and phase relationships to the 22-hr LD cycle are not stable. Of note, the same patterns of melatonin release could be simulated if the vlSCN passively responds to light and relays this information to the dmSCN and the pineal; yet, we have simulated the vlSCN as an oscillator because its increase in *Per1* expression persists in the absence of light on the first cycle after release into DD (16). A strikingly similar pattern of relative coordination was reported for locomotor activity in a spontaneously emerging mutant of *Peromyscus californicus* under a 24-h LD cycle, although the neural bases for this desynchronization are unknown (39).

Although similar patterns of melatonin release could be generated using independent oscillators that control the onset and offset of melatonin, we favor our more economical model, which does not require separate entrainment of melatonin onset and offset. We do not deny the validity of a dual-oscillator control model under other experimental conditions; however, we propose that, if present, these two oscillators do not dissociate under forced desynchronization and function as a single oscillator within the dmSCN.

The model predicts that upon release into DD light inhibition will cease and the output of the relative coordinated dm oscillator will be "unmasked." If an animal is released into DD from an aligned phase, in which the melatonin peak is long, the duration of the peak should remain long from the first cycle after release into DD (Fig. S1 *A* and *C*; projection schematized in Fig. S3*A*). If the cyclic narrowing of the melatonin peak under the LD22 is solely due to relative coordination of the dmSCN and masking, release into DD of an animal from a misaligned phase, in which the peak is compressed, should also result in an immediate increase of this peak's duration (projection schematized in Fig. S3*B*). However, our experimental results revealed that when release into DD occurred on misaligned phases, the melatonin bout was short on the first day and lengthened on successive days, showing true decompression dynamics (Fig. S1 *B* and *C*; projection schematized in Fig. S3*C*). This result invited us into a more careful observation of a feature of relative coordination, namely how the amplitude of an oscillator is affected by relative coordination.

Fig. 4*A* shows the periodic amplitude changes of the state variable of an oscillator during relative coordination. In the model, this amplitude could correspond to the concentration of a clock-gene product at the cellular level, or to an emergent oscillator state variable at the tissue level that underlies circadian periodicity of the rat. Because oscillator period changes evoke amplitude changes as well (40), amplitude varies periodically between maximum and minimum values during relative coordination (41) and minimum values occur on the misaligned day. Because in our model melatonin release occurs every time oscillator amplitude is above a threshold value, the bout duration therefore depends on the amplitude of the oscillator (Fig. 4 *B* and *C*). If the release into DD is started on a misaligned phase (day 2 in Fig. 4*A*), when oscillator amplitude is at a minimum and before the large phase delay, the melatonin bout will be short on the first DD cycle and will lengthen throughout successive cycles as the dm oscillator amplitude recovers slowly.

In summary, melatonin compression and decompression observed under forced desynchrony are due to three factors: (*i*) a melatonin onset delay relative to the 22-h LD cycle in subsequent days due to relative coordination (see below); (*ii*) masking of the melatonin offset by light; and (*iii*) the cyclic variation of the dm

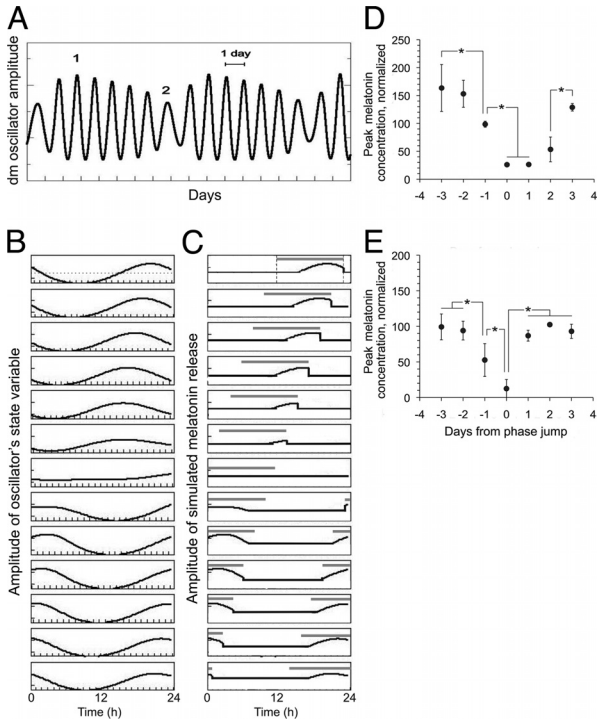

Fig. 4. Oscillator amplitude changes result from relative coordination and predict amplitude changes in melatonin release under forced desynchronization. (*A*) Periodic amplitude variation of variable S of oscillator dm under relative coordination. Release of system into DD on day "1" is expected to generate a wide melatonin bout on the first day in DD as schematized in Fig. S3*A*. Release into DD on day "2" is expected to generate a narrow melatonin bout on the first day in DD as schematized in Fig. S3*C*. (*B*) Amplitude changes are replotted as a 13-day actogram. (*C*) Simulation of output melatonin rhythm assuming that its amplitude is positively correlated to the amplitude of the dm oscillator and that is detectable when its value is above a threshold (dotted line in *B*). Finally, amplitude is set to zero during the light phase of the 22-h LD cycle starting at an arbitrary phase relationship to the oscillator (gray bars represent darkness). Parameters: $\tau_v = 23$ ($a_v = 0.85$; $b_v = 0.3$; $c_v = 1.1$; $d_v = 0.5$); $\tau_d = 24.3$ ($a_d = 0.85$; $b_d = 0.3$; $c_d = 0.75$; $d_d = 0.5$); $C_{vd} = 0.14$; $L_{dur} = 11$ h; $L = 1$; LD period $T = 22$ h). (*D* and *E*) The amplitude of the melatonin release rhythm is indeed reduced by the misalignment between forced desynchronized oscillators. Average melatonin peak amplitude on the days immediately before (−) and after (+) a phase jump designated as day 0, in Wistar (*D*) and Kyoto rats (*E*). To facilitate comparison between individuals, daily melatonin peak concentrations for each individual were normalized by dividing by the average of all daily peak values for that individual. *, $P < 0.05$.

oscillator's amplitude in relative coordination with a minimum during misaligned phases.

A prediction arose from our model, which was not obvious from the actogram representation of melatonin in Fig. 1. Amplitude changes of an output rhythm are positively or negatively correlated to amplitude changes of the underlying oscillator. Assuming a positive correlation between these two amplitudes, our model predicted that besides the suppression of melatonin release by lights on every 22 h, there would also be day-to-day amplitude variations in melatonin output, due entirely to the amplitude changes of dm oscillator under relative coordination (Fig. 4*A*). In Fig. 4*C* we show the predicted changes in the amplitude of melatonin release, separating explicitly melatonin suppression due to 22-h onset of light and changes in amplitude due to dm oscillator amplitude changes. Minimum amplitude levels of melatonin release should therefore occur on misaligned phases, and indeed our experimental data showed this was the case in both rat strains (Figs. 1*B* and 4 *C* and *D*). This prediction was also supported by the 5 animals released into DD, in which the amplitude showed a trend to be

smaller in those animals released from a misaligned phase than in those released from an aligned phase (one-tail t test, $P = 0.086$). Our model is also consistent with the reduced amplitude of AANAT levels observed after abrupt advances of the LD cycle (42); this amplitude reduction may reflect a decrease in the dm oscillator amplitude that in turn results from the transient desynchrony between the vl- and dmSCN after abrupt LD phase shifts (13, 38, 43).

Melatonin Waveform Under Forced Desynchronization. The model of melatonin temporal profiles under a forced desynchrony protocol is heavily based on the particular shape of oscillator waveforms in relative coordination. The zigzagging actogram pattern results from nearly entrained activity bouts that alternate with periodic large phase shifts. The origin of these large phase shifts has been debated for a long time in the context of spontaneous internal desynchronization (44, 45). Our simulation of an oscillator, with a hypothetical phase response curve, under relative coordination, predicts both these quasi-entrainment cycles and the large phase shifts (see *Output of an Oscillator under Relative Coordination* in *SI Text* and Fig. S4).

Both Wistar and Kyoto rats exhibit relative coordination of melatonin temporal profiles. However, two main differences can be detected: first, the activity bouts of Kyoto rats do not seem to be dissociated and second, the overall period of the non-entrained component is clearly shorter in Kyoto than in Wistar rats. This difference in dissociation between components and in overall period of the system can be simulated by changing a single parameter in our model, namely the strength of coupling between dm and vl (see *Strain Differences* in *SI Text* and Fig. S5).

Discussion

The organization of the SCN into its vl- and dmSCN subregions has been recognized based on criteria including neuroanatomical tract tracing, immunohistochemistry, and in situ hybridization (3). The functional heterogeneity of these subregions has been underscored by their differential response to light, and by their spontaneous oscillation of clock gene expression both in vivo and in vitro (4, 19). Their functional heterogeneity in regards to circadian output control has been more elusive. The 22-h LD forced desynchronization of these two subregions into a LD-associated vlSCN and a longer-period dissociated dmSCN offers an opportunity to assess the ability of these subregions to sustain independent circadian outputs. In these forced desynchronized rats, the rhythms of locomotor activity (15), as well as sleep stages and core body temperature (18) are internally desynchronized. These dissociated rhythms track independent oscillations of clock gene expression in the vl- and dmSCN (16, 17), suggesting that the dissociated SCN subregions act as independent pacemakers driving specific outputs. Here, we have capitalized on the forced desynchronized rat to dissociate two SCN-dependent regulatory limbs of melatonin synthesis, namely its circadian regulation and the ability of light to inhibit it. The result of this dissociation is a recurring pattern of successive compression of melatonin release followed by a large phase delay. Compression persisted upon release of forced desynchronized animals into DD when these releases occurred during phases at which the vl- and dmSCN oscillators were maximally misaligned, suggesting that these patterns are mediated via changes in pacemaker parameters and not merely via inhibition by light onset.

Based on these results, and on anatomical (9, 46) and functional (10, 13, 16, 38) observations of the SCN, we generated a mathematical model of the desynchronized SCN in the forced desynchronized rat. Under simulated 22-h LD cycles vl entrains to the LD cycle, but weak coupling between vl and dm, combined with the longer intrinsic period of dm, prevents full entrainment of dm. The resulting output pattern of relative coordination, with the addition of masking of melatonin release during the light phase, closely resembles the experimental melatonin profiles seen in forced desynchronized rats. In addition, the model accurately simulates an observed interstrain (Wistar vs. Kyoto) difference in the pattern of melatonin release. Finally, our model suggests that a single dm oscillator can control the asymmetric phase shifting of the melatonin onset and offset via relative coordination, changes in amplitude and masking. Together, these data indicate first, that the dmSCN controls the circadian melatonin profile and second, that the vlSCN is an oscillator that can both acutely inhibit melatonin release and entrain the dmSCN oscillator. Under 24-h LD cycles, the vlSCN is entrained; its weak coupling to the dmSCN and the proximity of Zeitgeber period to the dmSCN period result in entrainment of the dmSCN and the 24-h nocturnal rhythm of melatonin release (47).

In rats, efferent projections from the dm- and vlSCN project to distinct subsets of targets (9, 46, 48). Based on this topographic organization of projection neurons in the rat, Leak and Moore (9) have proposed that these subregions could govern distinct rhythmic outputs and thus constitute the basis for internal desynchronization of circadian rhythms. Our analysis of the rhythms of locomotor activity (16), sleep architecture, core body temperature (18) and —in the present study—melatonin release are in full agreement with this hypothesis. Axonal outputs from the SCN are necessary to sustain circadian neuroendocrine rhythms, including melatonin rhythms (49). Primary efferents from the SCN to the preautonomic PVN originate primarily from the dmSCN in rats (50–52) and hamsters (53), although a parallel vlSCN input is suggested by the presence of VIPergic fibers apposing preautonomic PVN neurons (51, 54). These tracing studies indicate that the dmSCN can be a source of circadian timing information to the pineal; in support of this, we observed that pineal melatonin release tracked the dissociated locomotor activity bout, which we show to be associated with the activity of the dmSCN in ref. 16. Simultaneously, the ability of light to acutely inhibit melatonin release was preserved and mirrored the previously described clock gene activity of the vlSCN under 22-h forced desynchronization. This is consistent with the presence of VIPergic innervation of the PVN (54) and the ability of SCN efferent neurons to be acutely stimulated by light in mice (55) and hamsters (56).

Masking is defined as an amplitude modulation of an output circadian rhythm due to processes downstream from the oscillator. Masking of melatonin by light, however, has challenged this definition because the SCN is necessary for its occurrence and it also contains the pacemaker that controls melatonin circadian release (30). According to our model the double role of the SCN in both the entrainment of the rhythm of melatonin release and its masking response to light (27), can be accounted for by its internal architecture as revealed by the forced desynchrony protocol. This architecture may also underlie excitatory and inhibitory neurochemical pathways that have been proposed to mediate the circadian and the light inhibition regulatory pathways of melatonin release (57).

Pittendrigh and Daan hypothesized that in nocturnal rodents, the onset and offset of circadian locomotor activity rhythms are coupled to separate light-entrainable circadian oscillators. These oscillators are phase-locked to the evening (oscillator E) and morning (oscillator M) light/dark transitions, and separate entrainment of these two oscillators under specific LD regimes can account for compression and decompression of the rhythms of locomotor activity (28, 29) and melatonin release, with onset and offsets phase-locked respectively to these two oscillators (30, 31, 58). However, according to our model, compression and decompression under forced desynchronization is not due to dissociation between these E and M oscillators. Instead, it is due to the dissociation between one oscillator within the dmSCN that controls circadian timing of melatonin and shows periodic amplitude changes, and another oscillator within the vlSCN that transmits light phase information necessary for entrainment and inhibition of melatonin release. Because coupled E and M oscillators are known to control

circadian timing of melatonin, we propose that in the rat they are both located in the dmSCN and remain synchronized under our forced desynchrony protocol. This interpretation is consistent with evidence of complex coexisting dual-oscillators within the SCN master pacemaker (59). Our results indicate that the subregional organization of the SCN is critical for the regulation of the two mechanisms—entrainment and masking—that restrict melatonin release to the night; they also highlight the complexity of the SCN neuronal network as a center for processing photic information.

Other rhythmic outputs in the forced desynchronized rat, including core body temperature, wakefulness and locomotor activity (18, 60), present patterns of relative coordination similar to those observed here for melatonin release. Furthermore, similar patterns were observed in other mammalian systems exposed to a weak Zeitgeber or one with a period near the limits of entrainment (61, 62). We propose a simple model that accurately reflects both the SCN's functional anatomy and empirical data on the regulation of its rhythmic outputs, and that offers experimentally testable predictions (see *Predictions of the Model* in *SI Text*). Our model offers an entrée to understanding how SCN subpopulations of single-cell oscillators interact with each other to master the regulation of rhythms throughout the body.

Methods

Male Kyoto–Wistar rats and Wistar rats were housed in LD 11:11 upon arrival to our laboratory until activity rhythms desynchronized (2–3 weeks). They were then implanted with transverse microdialysis probes during the light cycle and allowed to recover for at least 24 h. Online microdialysis began at 13:00 EST and continued without interruption for up to 20 days. Kyoto rats were maintained in LD 11:11 for the duration of the study. Wistar rats were monitored in LD 11:11 for 13 days, then released into DD and monitored for an additional 7 days. See *SI Materials and Methods*.

ACKNOWLEDGMENTS. We thank Chris Hart for his help in monitoring locomotor activity of rats and Lijun Wang for animal care. This work was supported by National Institutes of Health Grants R01MH075016 (to H.O.d.l.I.) and R01NS057583 (to J.B.) and Fundacao de Amparo a Pesquisa do Estado de São Paulo Grant 06/61276-0 (to G.A.O.).

1. Ralph MR, Foster RG, Davis FC, Menaker M (1990) Transplanted suprachiasmatic nucleus determines circadian period. *Science* 247:975–978.
2. Schwartz WJ (2002) Suprachiasmatic nucleus. *Curr Biol* 12:R644.
3. Moore RY, Speh JC, Leak RK (2002) Suprachiasmatic nucleus organization. *Cell Tissue Res* 309:89–98.
4. Silver R, Schwartz WJ (2005) The suprachiasmatic nucleus is a functionally heterogeneous timekeeping organ. *Methods Enzymol* 393:451–465.
5. Morin LP (2007) SCN organization reconsidered. *J Biol Rhythms* 22:3–13.
6. Ibata Y, et al. (1999) Functional morphology of the suprachiasmatic nucleus. *Frontiers in Neuroendocrinology* 20:241–268.
7. Morin LP, Allen CN (2006) The circadian visual system, 2005. *Brain Res Brain Res Rev* 51:1–60.
8. Moore RY, Lenn NJ (1972) A retinohypothalamic projection in the rat. *J Comp Neurol* 146:1–14.
9. Leak RK, Moore RY (2001) Topographic organization of suprachiasmatic nucleus projection neurons. *J Comp Neurol* 433:312–334.
10. Shigeyoshi Y, et al. (1997) Light-induced resetting of a mammalian circadian clock is associated with rapid induction of the mPer1 transcript. *Cell* 91:1043–1053.
11. Miyake S, et al. (2000) Phase-dependent responses of Per1 and Per2 genes to a light-stimulus in the suprachiasmatic nucleus of the rat. *Neurosci Lett* 294:41–44.
12. Yan L, Takekida S, Shigeyoshi Y, Okamura H (1999) Per1 and Per2 gene expresion in the rat suprachiasmatic nucleus: Circadian profile and the compartment-specific response to light. *Neuroscience* 94:141–150.
13. Nakamura W, Yamazaki S, Takasu NN, Mishima K, Block GD (2005) Differential response of Period 1 expression within the suprachiasmatic nucleus. *J Neurosci* 25:5481–5487.
14. Antle MC, Silver R (2005) Orchestrating time: Arrangements of the brain circadian clock. *Trends Neurosci* 28:145–151.
15. Campuzano A, Vilaplana J, Cambras T, Diez-Noguera A (1998) Dissociation of the rat motor activity rhythm under T cycles shorter than 24 hours. *Physiol Behav* 63:171–176.
16. de la Iglesia HO, Cambras T, Schwartz WJ, Diez-Noguera A (2004) Forced desynchronization of dual circadian oscillators within the rat suprachiasmatic nucleus. *Curr Biol* 14:796–800.
17. Lee ML, Swanson BE, de la Iglesia HO (2009) Circadian timing of REM sleep is coupled to an oscillator within the dorsomedial suprachiasmatic nucleus. *Curr Biol* 19:848–852.
18. Cambras T, et al. (2007) Circadian desynchronization of core body temperature and sleep stages in the rat. *Proc Natl Acad Sci USA* 104:7634–7639.
19. Schwartz WJ (2009) Circadian rhythms: A tale of two nuclei. *Curr Biol* 19:R460–462.
20. Moore RY, Klein DC (1974) Visual pathways and the central neural control of a circadian rhythm in pineal serotonin N-acetyltransferase activity. *Brain Res* 71:17–33.
21. Ganguly S, Coon SL, Klein DC (2002) Control of melatonin synthesis in the mammalian pineal gland: The critical role of serotonin acetylation. *Cell Tissue Res* 309:127–137.
22. Klein DC, Moore RY (1979) Pineal N-acetyltransferase and hydroxyindole-O-methyltransferase: Control by the retinohypothalamic tract and the suprachiasmatic nucleus. *Brain Res* 174:245–262.
23. Klein DC, et al. (1983) Lesions of the paraventricular nucleus area of the hypothalamus disrupt the suprachiasmatic leads to spinal cord circuit in the melatonin rhythm generating system. *Brain Res Bull* 10:647–652.
24. Cassone VM, Warren WS, Brooks DS, Lu J (1993) Melatonin, the pineal gland, and circadian rhythms. *J Biol Rhythms* 8 Suppl:S73–81.
25. Borjigin J, Wang MM, Snyder SH (1995) Diurnal variation in mRNA encoding serotonin N-acetyltransferase in pineal gland. *Nature* 378:783–785.
26. Roseboom PH, et al. (1996) Melatonin synthesis: Analysis of the more than 150-fold nocturnal increase in serotonin N-acetyltransferase messenger ribonucleic acid in the rat pineal gland. *Endocrinology* 137:3033–3045.
27. Redlin U (2001) Neural basis and biological function of masking by light in mammals: Suppression of melatonin and locomotor activity. *Chronobiol Int* 18:737–758.
28. Pittendrigh CS, Daan S (1976) Functional-analysis of circadian pacemakers in nocturnal rodents. 5. Pacemaker structure—clock for all seasons. *J Comp Physiol* 106:333–355.
29. Pittendrigh CS, Daan S (1976) Functional-analysis of circadian pacemakers in nocturnal rodents. 4. Entrainment—pacemaker as clock. *J Comp Physiol* 106:291–331.
30. Illnerova H, Vanecek J (1982) Two-oscillator structure of the pacemaker controlling the circadian rhythm of N-acetyltransferase in the rat pineal gland. *J Comp Physiol* 145:539–548.
31. Elliott JA, Tamarkin L (1994) Complex circadian regulation of pineal melatonin and wheel-running in Syrian hamsters. *J Comp Physiol A* 174:469–484.
32. Winfree AT (1967) Biological rhythms and the behavior of populations of coupled oscillators. *J Theor Biol* 16:15–42.
33. Pavlidis T (1969) Populations of interacting oscillators and circadian rhythms. *J Theor Biol* 22:418–436.
34. Enright JT (1980) Temporal precision in circadian systems: A reliable neuronal clock from unreliable components? *Science* 209:1542–1545.
35. Welsh DK, Logothetis DE, Meister M, Reppert SM (1995) Individual neurons dissociated from rat suprachiasmatic nucleus express independently phased circadian firing rhythms. *Neuron* 14:697–706.
36. Aton SJ, Herzog ED (2005) Come together, right now: Synchronization of rhythms in a mammalian circadian clock. *Neuron* 48:531–534.
37. Yan L, Okamura H (2002) Gradients in the circadian expression of Per1 and Per2 genes in the rat suprachiasmatic nucleus. *Eur J Neurosci* 15:1153–1162.
38. Nagano M, et al. (2003) An abrupt shift in the day/night cycle causes desynchrony in the mammalian circadian center. *J Neurosci* 23:6141–6151.
39. de Groot MH, Rusak B (2002) Entrainment impaired, masking spared: An apparent genetic abnormality that prevents circadian rhythm entrainment to 24-h lighting cycles in California mice. *Neurosci Lett* 327:203–207.
40. Winfree AT (1980) *The Geometry of Biological Time* (Springer, New York).
41. Wever RA (1972) Virtual synchronization towards the limits of the range of entrainment. *Journal of Theoretical Biology* 36:119–132.
42. Humlova M, Illnerova H (1990) Rate of re-entrainment of circadian rhythms to advances of light–dark cycles may depend on ways of shifting the cycles. *Brain Res* 531:304–306.
43. Albus H, Vansteensel MJ, Michel S, Block GD, Meijer JH (2005) A GABAergic mechanism is necessary for coupling dissociable ventral and dorsal regional oscillators within the circadian clock. *Curr Biol* 15:886–893.
44. Kronauer RE (1982) Modelling principles for human circadian rhythms. In *Mathematical Models of the Sleep–wake Cycle*, eds Moore-Ede MC, Czeisler CA (Raven, New York).
45. Eastman C (1982) Are separate temperature and activity oscillators necessary to explain the phenomena of human circadian rhythms? In *Mathematical Models of the Sleep–wake Cycle*, eds Moore-Ede MC, Czeisler CA (Raven, New York).
46. Leak RK, Card JP, Moore RY (1999) Suprachiasmatic pacemaker organization analyzed by viral transynaptic transport. *Brain Res* 819:23–32.
47. Liu TC, Borjigin J (2005) Free-running rhythms of pineal circadian output. *J Biol Rhythms* 20:430–440.
48. Watts AG, Swanson LW (1987) Efferent projections of the suprachiasmatic nucleus: II. Studies using retrograde transport of fluorescent dyes and simultaneous peptide immunohistochemistry in the rat. *J Comp Neurol* 258:230–252.
49. Meyer-Bernstein EL, et al. (1999) Effects of suprachiasmatic transplants on circadian rhythms of neuroendocrine function in golden hamsters. *Endocrinology* 140:207–218.
50. Vrang N, Larsen PJ, Moller M, Mikkelsen JD (1995) Topographical organization of the rat suprachiasmatic-paraventricular projection. *J Comp Neurol* 353:585–603.
51. Teclemariam-Mesbah R, Ter Horst GJ, Postema F, Wortel J, Buijs RM (1999) Anatomical demonstration of the suprachiasmatic nucleus-pineal pathway. *J Comp Neurol* 406:171–182.
52. Buijs RM, et al. (2003) The suprachiasmatic nucleus balances sympathetic and parasympathetic output to peripheral organs through separate preautonomic neurons. *J Comp Neurol* 464:36–48.
53. Kriegsfeld LJ, Leak RK, Yackulic CB, LeSauter J, Silver R (2004) Organization of suprachiasmatic nucleus projections in Syrian hamsters (Mesocricetus auratus): An anterograde and retrograde analysis. *J Comp Neurol* 468:361–379.
54. Teclemariam-Mesbah R, Kalsbeek A, Pevet P, Buijs RM (1997) Direct vasoactive intestinal polypeptide-containing projection from the suprachiasmatic nucleus to spinal projecting hypothalamic paraventricular neurons. *Brain Res* 748:71–76.
55. de la Iglesia HO, Schwartz WJ (2002) A subpopulation of efferent neurons in the mouse suprachiasmatic nucleus is also light responsive. *Neuroreport* 13:857–860.
56. Munch IC, Moller M, Larsen PJ, Vrang N (2002) Light-induced c-Fos expression in suprachiasmatic nuclei neurons targeting the paraventricular nucleus of the hamster hypothalamus: Phase dependence and immunochemical identification. *J Comp Neurol* 442:48–62.
57. Perreau-Lenz S, Kalsbeek A, Van der Vliet J, Pevet P, Buijs RM (2005) In vivo evidence for a controlled offset of melatonin synthesis at dawn by the suprachiasmatic nucleus in the rat. *Neuroscience* 130:797–803.
58. Liu T, Borjigin J (2005) Reentrainment of the circadian pacemaker through three distinct stages. *J Biol Rhythms* 20:441–450.
59. Gorman MR, Steele NA (2006) Phase angle difference alters coupling relations of functionally distinct circadian oscillators revealed by rhythm splitting. *J Biol Rhythms* 21:195–205.
60. Cambras T, Chiesa J, Araujo J, Diez-Noguera A (2004) Effects of photoperiod on rat motor activity rhythm at the lower limit of entrainment. *J Biol Rhythms* 19:216–225.
61. Richter CP (1977) Heavy water as a tool for study of the forces that control length of period of the 24-hour clock of the hamster. *Proc Natl Acad Sci USA* 74:1295–1299.
62. Rosenwasser AM, Boulos Z, Terman M (1983) Circadian feeding and drinking rhythms in the rat under complete and skeleton photoperiods. *Physiol Behav* 30:353–359.